Soil infiltration characteristics and pore distribution under freezing-thawing conditions

Ruiqi Jiang[1,2,3,★], Tianxiao Li[1,2,3,★], Dong Liu[1,2,3,*], Qiang Fu [1,2,3,*], Renjie Hou [1,2,3], Qinglin Li [1], Song Cui [1,2,3], Mo Li [1,2,3]

[1] School of Water Conservancy & Civil Engineering, Northeast Agricultural University, Harbin 150030, China

[2] Key Laboratory of Effective Utilization of Agricultural Water Resources of Ministry of Agriculture, Northeast Agricultural University, Harbin, Heilongjiang 150030, China

[3] Heilongjiang Provincial Key Laboratory of Water Resources and Water Conservancy Engineering in Cold Region, Northeast Agricultural University, Harbin, Heilongjiang 150030, China

*** Dong Liu and Qiang Fu are corresponding authors.**

★ These authors contributed equally to this work.

*Corresponding author at: School of Water Conservancy and Civil Engineering, Northeast Agricultural University, Harbin, Heilongjiang 150030, China

Correspondence to: liudong9599@yeah.net (Dong Liu). fuqiang0629@126.com (Qiang Fu)

Abstract. Frozen soil infiltration widely occurs in hydrological processes such as seasonal soil freezing and thawing, snowmelt infiltration, and runoff. Accurate measurement and simulation of parameters related to frozen soil infiltration processes are highly important for agricultural water management, environmental issues and engineering problems in cold regions. Temperature changes cause soil pore size distribution variations and consequently dynamic infiltration capacity changes during different freeze-thaw periods. To better understand these complex processes and to reveal the freeze-thaw action effects on soil pore distribution and infiltration capacity, black soils, meadow soils and chernozem were selected as test subjects, these soil types account for the largest arable land area in Heilongjiang Province, China. Laboratory tests of

soils at different temperatures were conducted using a tension infiltrometer and ethylene glycol aqueous solution. The stable infiltration rate and hydraulic conductivity were measured, and the soil pore distribution was calculated. The results indicated that for the different soil types, macropores, which constituted approximately 0.1% to 0.2% of the soil volume under unfrozen conditions, contributed approximately 50% of the saturated flow, and after soil freezing, the soil macropore proportion decreased to 0.05% to 0.1%, while the saturated flow proportion decreased to approximately 30%. Soil moisture froze into ice crystals inside relatively large pores, resulting in numerous smaller-sized pores, which reduced the number of macropores but increased the number of smaller-sized mesopores, so that the frozen soil infiltration capacity was no longer solely dependent on the macropores. After the ice crystals had melted, more pores were formed within the soil, enhancing the soil permeability.

Key words: Freezing-thawing soil; Hydraulic conductivity; Pore distribution; Macropores; Infiltration characteristics

1 Introduction

Over the last few decades, the temperature changes caused by global warming have altered the freezing state of near-surface soils, and in China, changes in characteristic values such as the extent of the mean annual area of the seasonal soil freeze/thaw state and maximum freezing depth, indicate the degradation of frozen soil, especially at high latitudes (Wang et al., 2019;Peng et al., 2016). Under the effect of temperature, most frozen regions experience seasonal freezing and thawing of soil, accompanied by coupled soil water and heat movement as well as frost heave processes, thus making the soil structure and function more variable (Oztas and Fayetorbay, 2003;Fu et al., 2019;Gao et al., 2018). Parameters such as the soil infiltration rate and hydraulic conductivity are key factors in the study of soil water movement, groundwater recharge, and solute and contaminant transport simulation (Angulo-Jaramillo et al., 2000). In regard to unfrozen soils,

46 temperature has been shown to change the soil structure and kinematic viscosity of soil water, thereby
47 affecting the unsaturated hydraulic conductivity of soils (Gao and Shao, 2015). In terms of frozen soils, the
48 water infiltration characteristics and pore size distribution are highly variable and difficult to observe
49 (Watanabe et al., 2013); moreover, the water movement in freezing-thawing soils is complicated by the
50 migration of water and heat and the associated water phase change (Hayashi, 2013). The accurate
51 measurement of water movement parameters and soil pore distribution under freeze-thaw conditions is a
52 necessary prerequisite for the quantitative description of the water movement in frozen soil, and the
53 mechanism and degree of influence of the temperature on the infiltration rate, hydraulic conductivity,
54 porosity and other parameters in the different stages of freeze-thaw periods require further research.
55 Currently, quantitative studies of the infiltration process in freezing-thawing soils can be mainly divided into
56 experimental and model studies. Field experiments have been performed less often because under natural
57 conditions, infiltration water exhibits a preferential flow into the deep soil, and the alternating freeze-thaw
58 effect forms ice crystals to block the flow path through large pores, subsequently limiting water infiltration
59 (Stadler et al., 1997), while the melting effect of the infiltration water on ice makes it difficult to reach a
60 steady infiltration state. Therefore, the current relevant achievements are mainly focused on the infiltration
61 process of snowmelt water (Hayashi et al., 2003) and the influence of preferential flow (Mohammed et al.,
62 2019). Controlled laboratory experiments provide new opportunities for the simulation of frozen soil
63 infiltration processes and the measurement of infiltration parameters. Williams and Burt (1974) conducted
64 early direct measurements in the laboratory, resolved the water freezing problem by adding lactose and
65 applied dialysis membranes on both sides of soil columns, and they determined the water conductivity of
66 saturated specimens in the horizontal direction (Burt and Williams, 1976). Andersland et al. (1996) measured
67 the hydraulic conductivity of frozen granular soils at different saturations using a conventional drop

permeameter with decane as the permeant and concluded that the hydraulic conductivity was the same as that of unfrozen soils with water as the infiltration solution. McCauley et al. (2002) determined and compared the differences in hydraulic conductivity, permeability and infiltration rate between frozen and unfrozen soils using diesel mixtures as permeants, and their results indicated that the ice content determines whether soil is sufficiently impermeable. Zhao et al. (2013) quantified the unsaturated hydraulic conductivity of frozen soil using antifreeze instead of water, adopted a multistage outflow method under controlled pressures and introduced the pore impedance coefficient. However, most of these studies did not consider the differences in kinematic viscosity and surface tension between soil water and other solutions, which often results in an overestimation of hydraulic conductivity, and homemade devices in the laboratory are often inconvenient for generalization in the field. Due to the dynamic changes in the temperature and moisture phase, direct measurement is difficult, and hydraulic conductivity empirical equations and models of frozen soil have been developed. First, the frozen soil hydraulic conductivity was simply considered to follow a power exponential relationship with the temperature (Nixon, 1991;Smith, 1985), while others considered the hydraulic conductivity of frozen soil to be equal to that of unfrozen soil at the same water content and assumed that the hydraulic conductivity of frozen soil was a function of the moisture content of unfrozen soil (Lundin, 1990;Flerchinger and Saxton, 1989;Harlan, 1973). On the basis of Campbell's model (Campbell, 1985), Tarnawski and Wagner (1996) proposed a frozen soil hydraulic conductivity model based on the soil particle size distribution and porosity. Watanabe and Wake (2008) viewed soil pores as cylindrical capillaries and suggested that ice formation occurs at the center of these capillaries and established a model to describe the movement of thin film water and capillary water in frozen soil based on the theory of capillaries and surface absorption (Watanabe and Flury, 2008). The similarity between freezing and soil moisture profiles has been demonstrated (Spaans and Baker, 1996;Spaans, 1994), and subsequently, soil freezing characteristic curves

have been applied to estimate the unsaturated hydraulic conductivity of frozen soils (Azmatch et al., 2012), which has been combined with field tests and inversion models to achieve a high accuracy (Cheng et al., 2019).

Understanding the distribution characteristics of the soil pore system is essential for the evaluation of the water and heat movement processes in soil. Soil macroporosity has been shown to impose a major impact on water cycle processes such as infiltration, nutrient movement and surface runoff. (Demand et al., 2019;Jarvis, 2007). Macroporosity is widespread in a variety of soils and produces preferential flow in both frozen and unfrozen soils (Mohammed et al., 2018;Beven and Germann, 2013), and the pre-freeze moisture conditions affect the amount and state of ice in the macropores of frozen soils, resulting in notable variability in the infiltration capacity of thawed soils (Hayashi et al., 2003;Granger et al., 1984). Field experiments on frozen soil have also demonstrated that macropores accelerate the infiltration rate (Stähli et al., 2004;Kamp et al., 2003), the number and size of macropores affect the freezing and infiltration capacity of soil layers to different extents, and low temperatures cause infiltration water to refreeze inside macropores (Watanabe and Kugisaki, 2017;Stadler et al., 2000). Research on frozen soil macroporosity has largely focused on the qualitative analysis of its impact on the soil structure and infiltration capacity, and with the development of experimental techniques, certain new methods and techniques, such as computed tomography (CT) and X-ray scanning, have been applied to measure the number and distribution of macropores (Taina et al., 2013;Bodhinayake et al., 2004;Grevers et al., 1989), but the lack of sampling techniques targeting frozen soil still restricts related research.

Many limitations and deficiencies remain in the direct measurement of frozen soil infiltration characteristics and pore distribution, and the relevant models also require a large amount of measured data to meet the accuracy and applicability requirements. In this paper, the stable infiltration rate and hydraulic conductivity

of three types of soils at different temperatures were measured by precise control of the soil and ambient temperatures, and the macropore and mesopore size distribution was calculated by using a tension infiltrometer and a glycol aqueous solution as the infiltration medium. The conclusions provide a basis and reference for the numerical simulation of the coupled water-heat migration process of freezing-thawing soil and related parameterization studies.

2 Materials and methods

2.1 Test plan

Referring to arable land area data of various regions of Heilongjiang Province, the three types of soils that dominate the cultivated land area in this province are black soils, meadow soils and chernozem (Bureau, 1992). Harbin, Zhaoyuan and Zhaozhou were selected as typical soil areas for sampling. A 5-cm surface layer of floating soil and leaves was removed, and topsoil samples were collected at depths ranging from 0-20 cm. After natural air drying and artificial crushing, the soil was sieved, and particles larger than 2 mm in diameter were removed. The remainder was used to prepare soil columns. The basic physical and chemical parameters of the test soils, such as the bulk density, organic content and mechanical parameters, are listed in Table 1.

An artificial climate chamber was applied to control the temperature of the soil column and infiltration solution, and four temperature treatments were established with three replications for each treatment: 15°C, unfrozen soil, representing the soil before freezing, which was recorded as 15°C (BF); -5°C, stable freezing; -10°C, stable freezing; and freezing at -10°C followed by thawing at 15°C, representing the soil after melting, which was recorded as 15°C (AM). Each soil column was tested for only one treatment. The freezing and thawing times were both 48 h. When the soil temperature was consistent with the set temperature in the climate chamber, the samples were considered to be completely frozen, and the effect of the number of

freezing and thawing cycles was not considered in this test. According to the basic information of the original soil, the volumetric moisture content of the sieved soil was set to 30%±2% using deionized water, with a dry bulk density of 1.2 g/cm^3. The soil porosity and pre-freezing soil water content of the repacked samples are shown in Table 2.

Table 1

Basic physical and chemical properties of three kinds of soils

Soil types	Bulk density (g/cm^3)	Organic content (g/kg)	Electrical conductivity (s/m)	Particle size (sand-silt-clay) (%)	Soil texture
Black soil	1.31	28.32	0.02	12.64-70.82-16.54	
Meadow soil	1.22	16.51	0.01	9.52-73.00-17.48	silt loam
Chernozem	1.15	26.52	0.01	38.99-50.30-10.71	

Table 2

Soil porosity and pre-freezing soil water content of repacked samples

Soil types	Soil porosity (%)	Pre-freeing water content (%)	
		-5°C	-10°C
Black soil	52.76	30.53	29.27
Meadow soil	52.82	29.83	30.70
Chernozem	53.22	30.07	30.93

To ensure a homogeneous column, the soil was loaded into a polyvinyl chloride (PVC) cylinder at 5-cm depth intervals, and petroleum jelly was applied to the sides to reduce the sidewall flow (Lewis and Sjöstrom, 2010). The PVC cylinder was 26 cm in diameter and 30 cm in height, with a perforated plate at the bottom. To prevent lateral seepage, the barrel occurred 5 cm above the soil surface, and the thickness of the soil layer

was 20 cm. A HYDRA-PROBE II sensor (STEVENS Water Monitoring Systems, Inc., Portland, Oregon, USA) was inserted in the middle of the barrel to observe the potential soil temperature and liquid water content change to determine whether ice melting occurred, and the ice content of frozen soil was measured by the drying method. A 5-cm thick layer of sand and gravel was placed below the soil column, and a 5-cm thick layer of black polypropylene insulation cotton was wrapped around the outer layer and the bottom of the soil column. The stable infiltration rate under tension levels of -3, -5, -7, -9, -11, and -13 cm was measured with a tension infiltrometer, and the infiltration time and cumulative infiltration were recorded. The detailed layout of the test apparatus is shown in Fig. 1.

The addition of a certain amount of lactose, antifreeze or other substances to water greatly reduces the freezing point of water (Zhao et al., 2013;Williams and Burt, 1974) so that the soil macropores are not quickly filled with ice with decreasing temperature, thereby maintaining better conditions for water flow. To further verify the feasibility of the use of deionized water to prepare an aqueous solution of ethylene glycol at a mass concentration of 40% as the infiltration medium for the frozen soil measurements, the surface tension of the aqueous glycol solution at -5°C and -10°C and its relationship with the temperature were measured with a contact angle measuring instrument (OCA20, DataPhysics Instruments, Germany) and a surface tension measuring instrument (DCAT-21, DataPhysics Instruments, Germany), respectively. As an example, the contact angle measurement process of the black soil at -10°C with the aqueous ethylene glycol solution is shown in Fig. 2, and it is observed that the contact angle decreases to 0° within a few seconds after the liquid droplet is placed on the soil, and the liquid droplet completely dissolves in the frozen soil, which implies that the addition of glycol to water does not alter the wetting ability of the soil particles (Lu and Likos, 2004). The relevant physicochemical properties of the aqueous ethylene glycol solution and water are compared in Table 3.

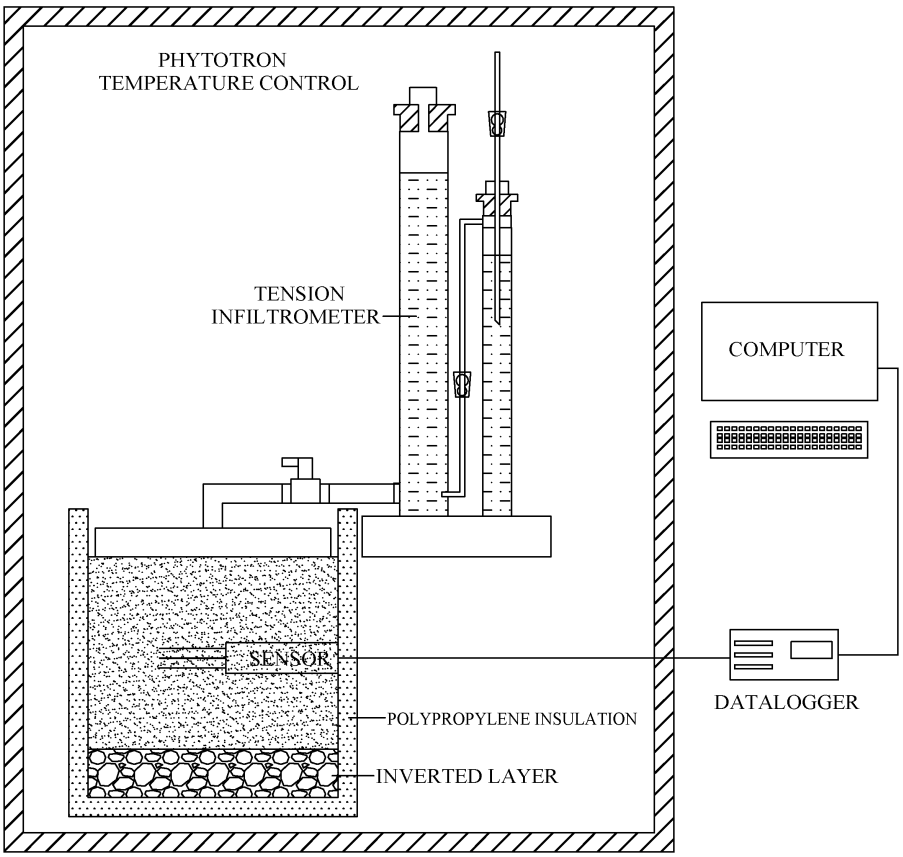

168

169 **Fig. 1**. Diagram of the test equipment.

170

171 **Fig. 2**. Process of the contact angle measurement between the aqueous ethylene glycol solution and black

172 soil at -10°C.

173 **Table 3**

174 **Comparison of the physicochemical properties of the 40% ethylene glycol aqueous solution and**

175 **water**

Infiltration solution	Temperature (°C)	Density (g/cm^3)	Dynamic viscosity (mPa.s)	Surface tension (mN/m)	Contact angle (°)

Water	15	0.9991	1.14	73.56	0
Ethylene glycol	-5	1.0683	7.18	48.89	0
aqueous solution	-10	1.0696	9.06	49.10	0

2.2 Measurement of the frozen soil hydraulic conductivity

Gardner (1958) proposed that the unsaturated hydraulic conductivity of soil varies with the matric potential as follows:

$$K(h) = K_{sat}\exp(\alpha h) \quad (1)$$

where K_{sat} is the saturated hydraulic conductivity, cm/hour, and h is the matric potential or tension, cm H_2O. Wooding (1968) considered that the steady-state unconfined infiltration rate into soil from a circular water source of radius R can be calculated with the following equation:

$$Q = \pi R^2 K\left[1+\frac{4}{\pi R\alpha}\right] \quad (2)$$

where Q is the amount of water entering the soil per unit time, cm^3/h; K is the hydraulic conductivity, cm/hour; and α is a constant. Ankeny et al. (1991) proposed that implementing two successively applied pressure heads h_1 and h_2 could yield the unsaturated hydraulic conductivity, and upon replacing K in Eq. (2) with Eq. (1), the following is obtained:

$$Q(h_1) = \pi R^2 K_{sat}\exp(\alpha h_1)\left[1+\frac{4}{\pi R\alpha}\right] \quad (3)$$

$$Q(h_2) = \pi R^2 K_{sat}\exp(\alpha h_2)\left[1+\frac{4}{\pi R\alpha}\right] \quad (4)$$

Dividing Eq. (4) by Eq. (3) and solving for α yields:

$$\alpha = \frac{\ln[Q(h_2)/Q(h_1)]}{h_2 - h_1} \quad (5)$$

where $Q(h_1)$ and $Q(h_2)$ can be measured, h_1 and h_2 are the preset tension values, and α can be calculated with

193 Eq. (5). The result can be substituted into Eq. (3) or (4) to calculate K_{sat}. When the number of tension levels
194 is higher than 2, parameter fitting methods can be applied to improve the accuracy of α and K_{sat} (Hussen and
195 Warrick, 1993).
196 The tension is controlled by the bubble collecting tube of the tension infiltrometer, and different pressure
197 heads h correspond to different pore sizes r. By applying different pressure heads h to the soil surface, water
198 will overcome the surface tension in the corresponding pores and will be discharged, and the infiltration
199 volume is recorded after reaching the stable infiltration state.
200 Under the assumption that the frozen soil pore ice pressure is equal to the atmospheric pressure and that
201 solutes are negligible, the Clausius-Clapeyron equation can be adopted to achieve the interconversion
202 between the soil temperature and suction (Konrad and Morgenstern, 1980;Watanabe et al., 2013), which can
203 be simplified as follows:

204 $$\psi = -L\rho_w \frac{T}{273.15} \quad (6)$$

205 where ψ is the soil suction, kPa; L is the latent heat of fusion of water, 3.34×10^5 J/kg; ρ_w is the density of
206 water, 1 g/cm^3; and T is the subfreezing temperature, °C. After the unit conversion of the soil suction into h
207 (cm H_2O), the unsaturated hydraulic conductivity of frozen soil at different negative temperatures can be
208 obtained via substitution into Eq. (2).

209 **2.3 Measurement of the pore size distribution in frozen soil**

210 As a nonuniform medium, soil consists of pores with various pore sizes, and the equation for the soil pore
211 radius r can be obtained from the capillary model (Watson and Luxmoore, 1986):

212 $$r = -\frac{2\sigma\cos\beta}{\rho g h} \quad (7)$$

213 where σ is the surface tension of the solution, g/s^2; β is the contact angle between the solution and pore wall;

214 ρ is the density of the solution, g/cm^3; g is the acceleration of gravity, m/s^2; and h is the corresponding tension

215 of the tension infiltrometer, cm H_2O.

216 The effective macroporosity θ_m can be calculated for various soil particle sizes based on the Poiseuille

217 equation (Wilson and Luxmoore, 1988):

218 $$\theta_m = 8\mu K_m / \rho g r^2 \quad (8)$$

219 where μ is the dynamic viscosity of the fluid, g/(cm*s); K_m is the macropore hydraulic conductivity and is

220 defined as the difference between K(h) at various tension gradients, cm/h; and r is the corresponding

221 equivalent pore size. The effective porosity is equal to the number of pores per unit area multiplied by the

222 area of the corresponding pore size. For different pore sizes, the maximum number of effective macropores

223 per unit area N can be calculated with the following equation:

224 $$N = \theta_m / \pi r^2 \quad (9)$$

225 where N is the number of effective macropores per unit area, and Eq. (7) calculates the minimum value of

226 the pore radius, while the result obtained with Eq. (9) is actually the maximum number of effective

227 macropores per unit area and the maximum porosity.

228 Considering the differences in surface tension and density between the aqueous ethylene glycol solution and

229 water, when calculating the frozen soil pore size distribution, it is necessary to convert the tension into the

230 equivalent pore radius according to Eq. (7), which is classified and subdivided into large and medium pores

231 according to the common classification method (Luxmoore, 1981), the details of which are listed in Table 4,

232 while the corresponding tension values in Table 4 are substituted into the fitting curve equation to calculate

233 the corresponding stable infiltration rate q and unsaturated hydraulic conductivity K.

234 **Table 4**

235 **Tension and equivalent pore radius conversions**

Pore types	Pore radius (mm)	Tension conversion (cm)		
		Water (15℃)	Ethylene glycol aqueous solution (-5℃)	Ethylene glycol aqueous solution (-10℃)
Macroporous	>0.5	0~3	0~1.86	0~1.87
Mesoporous	0.3-0.5	3~5	1.86 ~3.11	1.86 ~3.12
	0.15-0.3	5~10	3.11~6.22	3.12~6.23
	0.1-0.15	10~15	6.22~9.32	6.23~9.35
	0.05-0.1	15~30	9.32~18.65	9.35~18.70

3 Results

3.1 Infiltration characteristics of freezing-thawing soils

Curves of the recorded cumulative infiltration and infiltration rate were plotted over time, as shown in Figs. 3 and 4, respectively. The unfrozen water contents and ice contents of the frozen samples are shown in Table 5. The constant α and saturated hydraulic conductivity K_{sat} were calculated under different tensions h and corresponding steady-state infiltration rates q, and the unsaturated hydraulic conductivity under different tensions was calculated with Eq. (1). The stable infiltration rate and unsaturated hydraulic conductivity at different temperatures are shown in Fig. 5, and the details of α and K_{sat} are listed in Table 6.

Table 5

Unfrozen water contents and ice contents of the frozen samples

Soil types	Unfrozen water contents (cm^3/cm^3)		Ice contents (cm^3/cm^3)	
	-5℃	-10℃	-5℃	-10℃
Black soil	0.123	0.101	0.159	0.179
Meadow soil	0.128	0.109	0.145	0.167
Chernozem	0.119	0.097	0.151	0.185

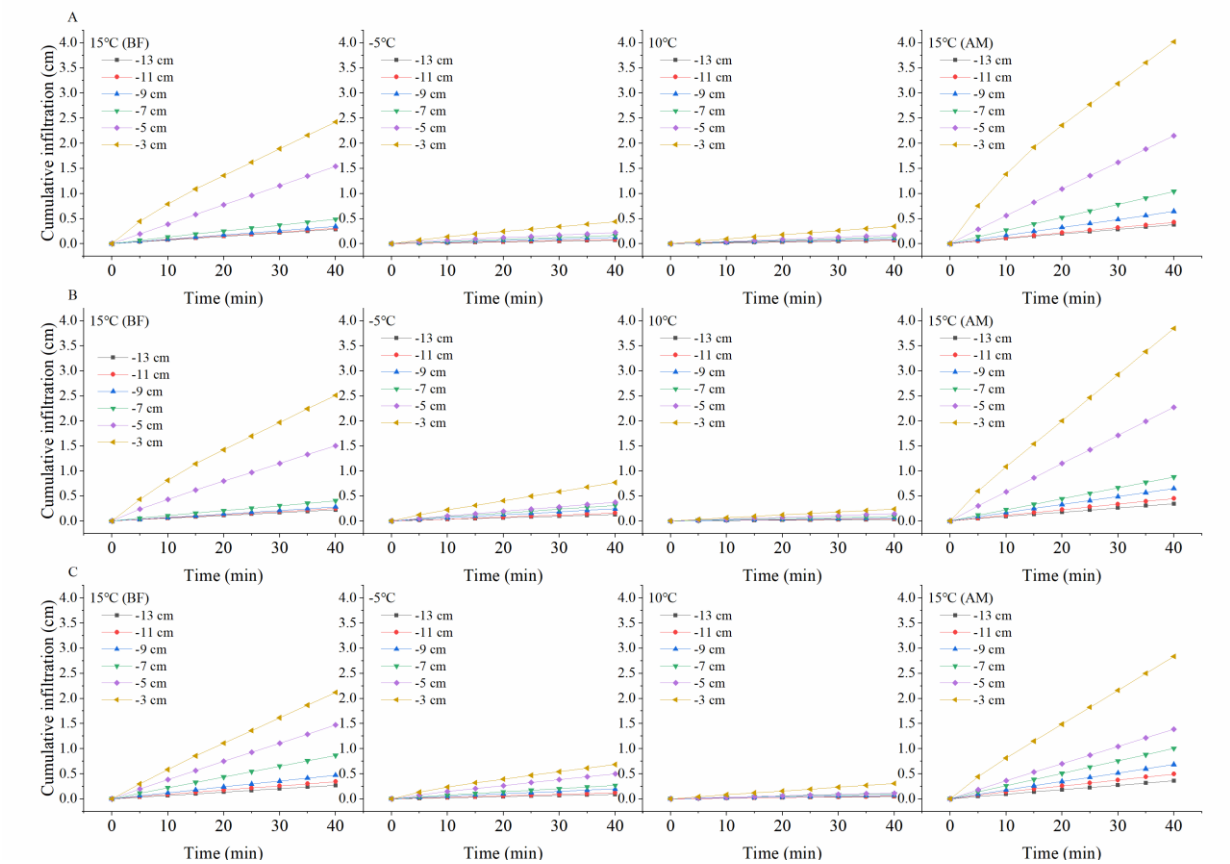

Fig. 3. Cumulative infiltration over time under the different treatments.

Note: A Black Soil; B Meadow Soil; C Chernozem.

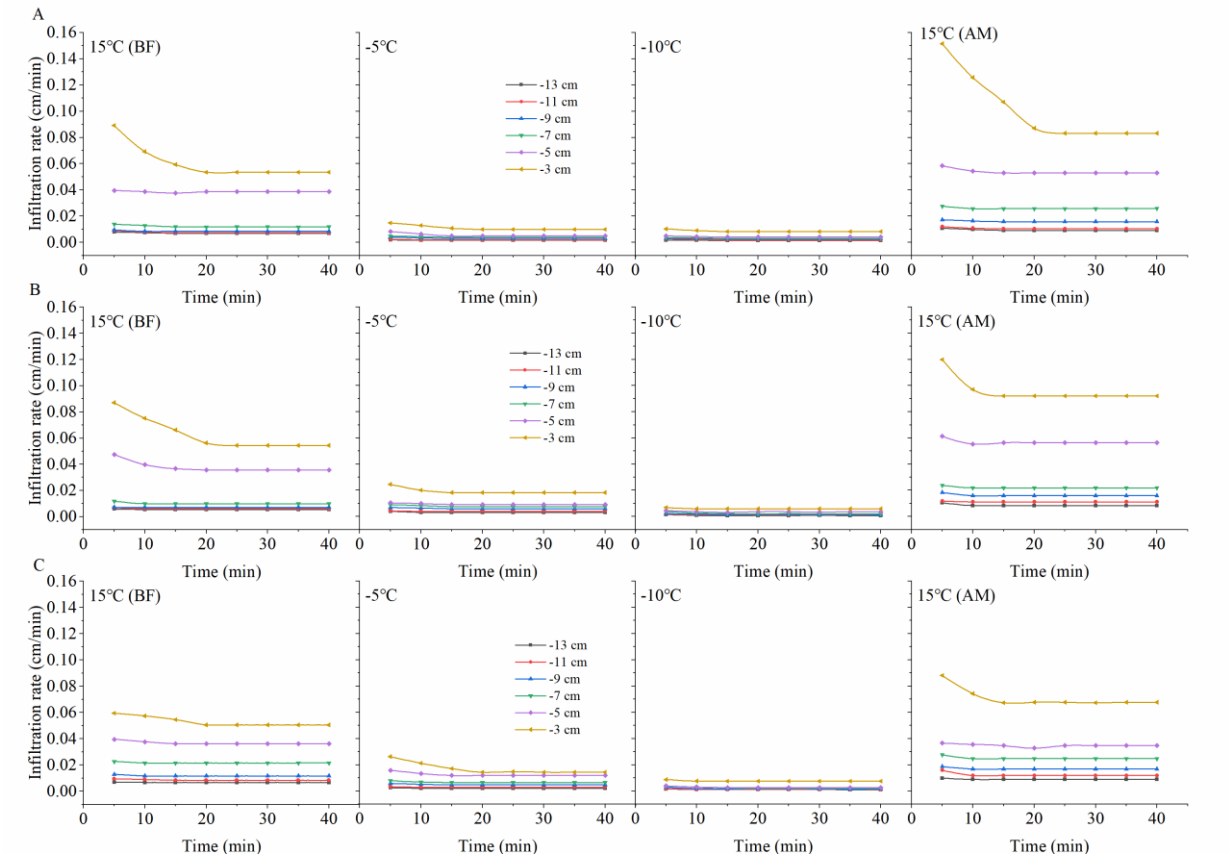

Fig. 4. Infiltration rate over time under the different treatments.

Note: A Black Soil; B Meadow Soil; C Chernozem.

As shown in Figs. 4 and 5, under the different tension conditions, the infiltration capacity of the unfrozen soil is basically consistent with the findings of field experiments and is highly influenced by the tension value (Wang et al., 1998). Compared to the room-temperature soil, the cumulative infiltration of frozen soil slowly increases, and the infiltration rate always remains low, while under the same negative temperature treatment, the influence of the tension value is also greatly reduced. When the temperature was reduced to -10°C, few major tension differences were observed except for the maximum tension of -3 cm. Based on the change in the slope of the two curves, the time for the unfrozen soil to reach the stable infiltration rate usually ranges from 15~20 min, while the time for the frozen soil to reach the stable infiltration rate is usually 10 min under higher tensions of -3 and -5 cm and 5 min under lower tensions. A comparison of the infiltration process before and after the freezing and thawing of the soil indicates that overall, the cumulative infiltration

and infiltration rate exhibited varying degrees of increase with increasing tension value, and the increase amplitude expanded. Moreover, the difference in the cumulative infiltration and infiltration rate between the low tension levels ranging from -9 to -13 cm after soil thawing was larger than that before soil freezing, which also indirectly demonstrated that freezing and thawing could further stabilize the soil pore distribution by affecting the homogeneity, which will be detailed in subsequent sections.

Table 6

Infiltration parameters of the different temperature treatments of the three soil types

Soil types	Temperature (℃)	α (cm/h)	K_{sat} (cm/h)
Black soil	15 (BF)	0.2742	5.1480
	-5	0.1993	0.5960
	-10	0.2028	0.5221
	15 (AM)	0.2629	7.4658
Meadow soil	15 (BF)	0.3071	5.9232
	-5	0.1996	1.1385
	-10	0.2477	0.4903
	15 (AM)	0.2934	9.3757
Chernozem	15 (BF)	0.2166	3.7185
	-5	0.1907	0.9739
	-10	0.2508	0.6077
	15 (AM)	0.2182	5.1283

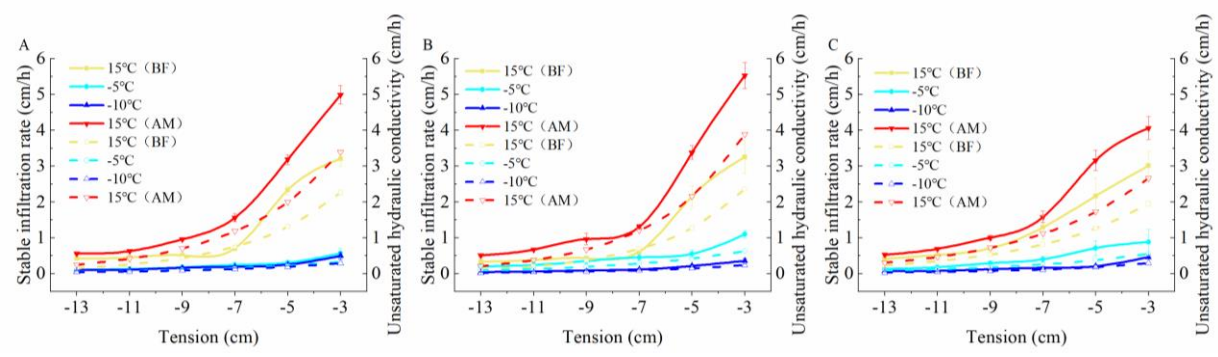

Fig. 5. Variation curves of the unsaturated hydraulic conductivity and stable infiltration rate with the tension for the different treatments of the three soils.

Note: A Black soil; B meadow soil; C chernozem. The solid lines represent the stable infiltration rate, and the dashed lines represent the unsaturated hydraulic conductivity.

By combining Fig. 5 and Table 6, we observe that the three types of soils exhibit a high infiltration capacity under normal temperature conditions. With increasing set tension value, the suction force of the soil matrix gradually weakened, the constraint and maintenance capacity of the matric potential with respect to the soil water decreased, the number of pores involved in the soil water infiltration process increases, and the unsaturated hydraulic conductivity and stable infiltration rate of the three types of soils exhibited different degrees of increase. When the temperature was lowered from 15℃ to -5℃ and the soil reached the stable frozen state, the saturated water conductivity of the black soil, meadow soil and chernozem soil decreased by 88.42%, 80.78% and 73.8%, respectively. When the soil temperature was decreased to -10 ℃, due to the presence of liquid water in the pores, the saturated water conductivity still exhibited a certain decrease over the pre-freeze conditions and continued to decrease by 1.43%, 10.94% and 9.85%, respectively. At negative temperatures, the unsaturated hydraulic conductivity decreased considerably and fluctuated within a small range, mainly because the unfrozen water content and saturated hydraulic conductivity were low after soil freezing. Based on a comparing of the -5℃ and -10℃ treatments, the unsaturated hydraulic conductivity (ANOVA, $P=0.72$, $F=0.14$) and stable infiltration rate (ANOVA, $P=0.71$, $F=0.15$) of the black soil exhibited almost no significant change, indicating that most of its pores were filled with ice crystals at -5℃ and were no longer involved in water infiltration. The unsaturated water conductivity of the meadow and chernozem soils still exhibited a more significant reduction when the freezing temperature was further reduced to -10℃. When the temperature was raised again to 15℃ and the soil was completely thawed, the steady infiltration

rate and saturated hydraulic conductivity increased with increasing temperature, and the values were higher than those of the soil at the same temperature before freezing. The saturated hydraulic conductivity of the black soil, meadow soil and chernozem increased by 45.02%, 58.63% and 37.91%, respectively, relative to the 15℃ (BF) treatment values.

3.2 Pore distribution characteristics of the freezing-thawing soil

Considering the differences in the physical and chemical properties between the infiltration solutions, infiltration parameters such as the hydraulic conductivity and stable infiltration rate alone do not fully reflect the infiltration characteristics and internal pore size of frozen soils. According to Eqs. (7)-(9), the maximum number per unit area N, effective porosity θ_m and percentage of pore flow to saturated flow P corresponding to the different soil pore sizes of the three soils under the different temperature treatments were calculated, as shown in Figs. 6 and 7.

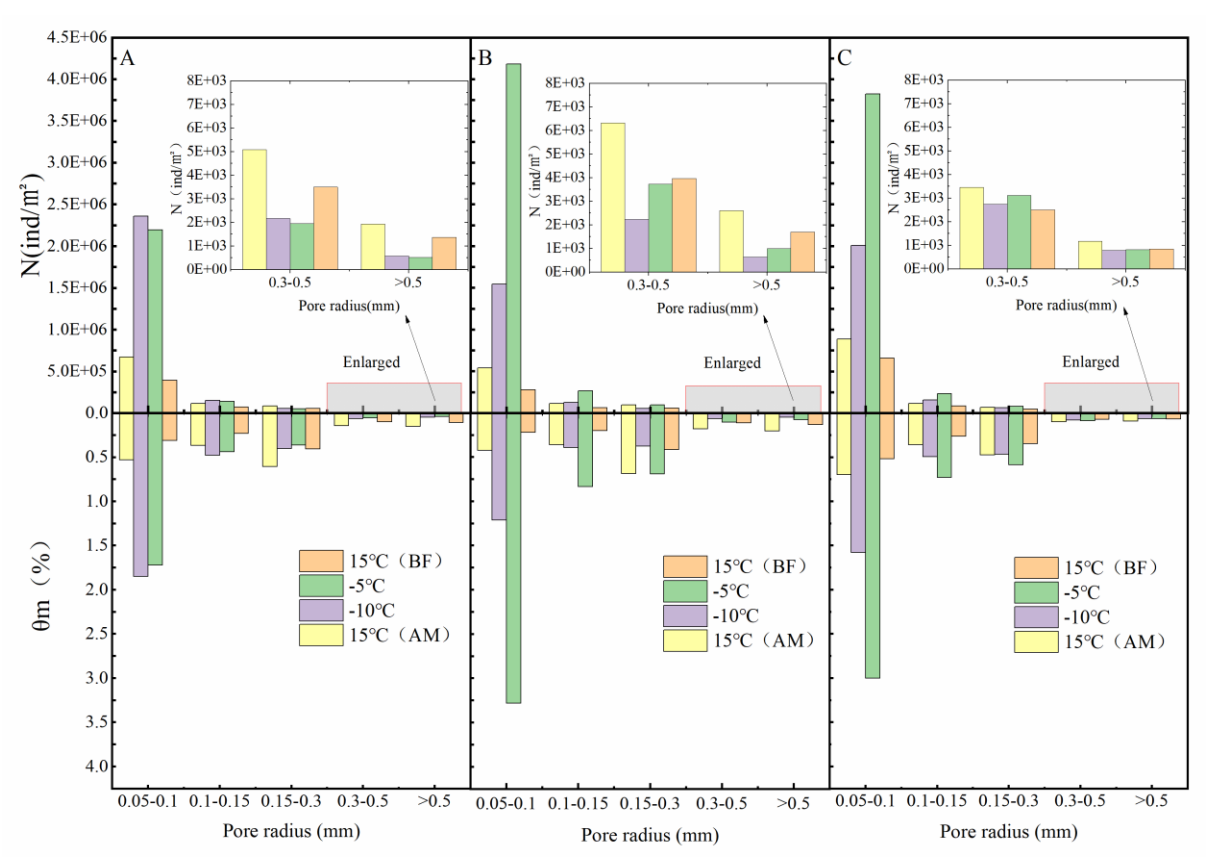

Fig. 6. Number of pores and effective porosity of the different equivalent pores.

309 Note: A Black Soil; B Meadow Soil; C Chernozem.

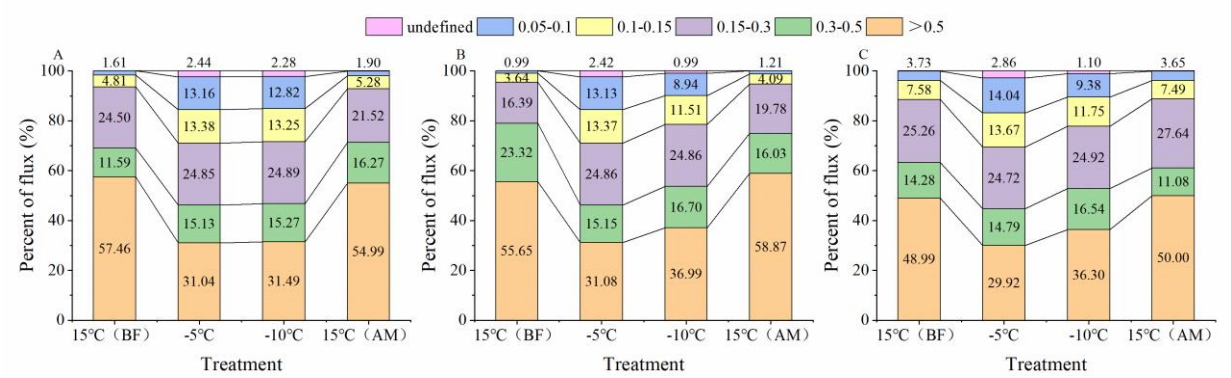

310

311 **Fig. 7**. Percentage of the pore flow in the saturated flow for the different equivalent pore sizes.

312 Note: A Black Soil; B Meadow Soil; C Chernozem.

313 Fig. 6 shows that pores of different equivalent radii widely occur in all three soils, and under all four
314 temperature treatments, the largest N value is that for the medium pores with an equivalent radius of 0.05-
315 0.1 mm, and N gradually decreases with increasing equivalent radius size. Under the two room-temperature
316 treatments at 15°C (BF) and 15°C (AM), the largest number of 0.05- to 0.1-mm medium pores and the
317 smallest number of >0.5-mm macropores differed by two orders of magnitude, and the number of pores of
318 each size exhibited different degrees of increase or decrease in the two treatments at -5°C and -10°C where
319 freezing occurred, with the number of medium pores with an equivalent pore size of 0.05-0.1 mm
320 significantly changing. Increases of more than an order of magnitude were achieved in all three soils, while
321 the macropores with an equivalent pore size of >0.5 mm were generally reduced by an order of magnitude,
322 with the difference in the number of pores of these two sizes reaching four orders of magnitude. This
323 indicates that freezing caused by temperature change significantly alters the soil internal structure, with ice
324 crystals forming in the relatively large pores containing the internal soil moisture, resulting in a large number
325 of smaller pores. Based on an assessment of the two treatments at -5°C and -10°C separately, when the
326 temperature was lowered from -5°C to -10°C, the number of pores in each pore size interval of the meadow

and chernozem soils exhibited a significant decrease, while the black soil revealed a small increase, which might be related to the high organic matter content of the black soil. A comparison of the two treatments at 15℃ (BF) and 15℃ (AM) indicated that the number of pores in all three soils increased to different degrees after thawing, and more pores were formed with the melting of ice crystals after the freeze-thaw destruction of the soil particles, which enhanced the soil water conductivity.

Comprehensive analysis of Figs. 6 and 7 reveals that before freezing, the θ_m values of the various pore sizes of the black soils, meadow soils and chernozem with an equivalent radius of >0.5 mm were 0.11%, 0.13% and 0.07%, respectively, while the P value reached 57.46%, 55.65% and 48.99%, respectively, with the values of the thawed soil similar to these values. This indicates that for all five soil pore sizes under unfrozen conditions, although the number of macropores with a pore size >0.5 mm was the smallest and the effective porosity was the lowest, their contribution to the saturated flow was usually more than half, and the macropores needed to represent only a small fraction of the pore volume to significantly contribute to the soil water flow. For the frozen soil, the P value of the >0.5-mm macropores was significantly reduced and remained at approximately 30% after the reduction, while the P value of the smaller pore sizes such as 0.15-0.3 mm, 0.1-0.15 mm, and 0.05-0.1 mm, revealed different degrees of increase. Moreover, the smaller the pore size, the greater the P value increased, and the contribution of these pores eventually accounted for more than 10% of the saturated flow. The saturated flow became more evenly distributed across the pores of each size, and the total proportion of medium pores exceeded that of the macropores. This indicates that the freezing action caused obvious changes to the soil structure, pore size and quantity, and although the macropores still played an important role, the infiltration capacity of the frozen soil no longer relied solely on these macropores, and the contribution of certain smaller-sized mesopores to the infiltration capacity of the frozen soil could no longer be neglected. Selecting black soil as an example, the total effective porosity

of the pores of each size under the four treatments was 1.15%, 2.62%, 2.84%, and 1.80%, and the P values were 99.97%, 97.56%, 97.72%, and 99.96%, respectively, which implies that the soil water infiltrated almost entirely via the large and medium pores. The small micropores, even in large numbers, contributed little to the infiltration process.

4 Discussion

4.1 Permeability and hydraulic conductivity of the frozen soil

It is worth noting that the theory underpinning the tension infiltration analysis in this article is based on the assumption that larger pores only flow fully saturated which means no air-water interface inside the pore and excludes the formation of an air-water interface with flowing water in larger pores (Perroux and White, 1988). However, recent work has shown that this flow mode does indeed occur (Beven and Germann, 2013;Nimmo, 2012, 2010).

In the field environment, although it is difficult to accurately measure the infiltration rate of frozen soils using traditional instruments and methods such as single-loop infiltrators, the obtained test results still demonstrate that the infiltration capacity decreases by one or more orders of magnitude when the soil is frozen (Stähli et al., 2004). Although the cumulative infiltration and infiltration rate of frozen soil are low, the presence of unfrozen water allows a certain amount of infiltration flow to be maintained in the soil. When water is applied as the infiltration solution, the low temperature of the frozen soil easily causes the infiltration water to freeze, thus forming a thin layer of ice on the soil particle surface and delaying the subsequent infiltration of water. This phenomenon results in a low infiltration rate after the freezing of soils with a high initial water content and a relatively high infiltration rate after the freezing of dry soils (Watanabe et al., 2013), because the higher the ice content is, the more latent heat needs to be overcome to melt any ice crystals, resulting in a weakened propagation of the melting front, thus limiting the infiltration rate so that it is

controlled by the downward movement of the melting leading edge of the ice crystals (Pittman et al., 2020). During the measurements using the tension infiltrator in this study, the sensor temperature always remained consistent with the soil temperature, indicating that the use of an aqueous glycol solution could be a useful way to avoid the problem of freezing of the infiltration solution. In addition, the hydraulic conductivity of frozen soils with different capacities and at various water flow rates was demonstrated not to greatly differ (Watanabe and Osada, 2017).

Whether water or other low-freezing point solutions are applied as infiltration media, the hydraulic conductivity of frozen soil significantly changes only within a limited temperature range above -0.5°C depending on the unfrozen water and ice contents, and at a soil temperature below -0.5°C, the hydraulic conductivity usually decreases to less than 10^{-10} m/s (Watanabe and Osada, 2017;Williams and Burt, 1974). The unsaturated hydraulic conductivity in our experiments was measured at a set tension level, and according to Eq. (6), the soil substrate potential increases by 125 m for every 1°C decrease in temperature (Williams and Smith, 1989), while the frozen soil hydraulic conductivity calculated at -5°C and -10°C, which corresponds to the actual matric potential, is much lower than 10^{-10} m/s and can be ignored. This suggests that even under ideal conditions where no heat exchange occurs between the infiltration solution and the soil and no freezing of the infiltration water takes place to prevent subsequent infiltration, the unsaturated hydraulic conductivity of frozen soil is so low that the frozen soil at lower temperatures in its natural state could be considered impermeable, with respect to both water and other solutions.

4.2 Effect of freeze-thaw cycles on soil pore distribution

In our study, the N value after freezing for the different types of soil was approximately 1000-2000/m^2 base on the tension infiltrator, which agreed well with other studies and remained at a same magnitude (Pittman et al., 2020), indicating that the method is generally reliable. The freeze-thaw effect significantly improves

393 the water conductivity of the different types of soils because it increases the porosity, decreases the soil
394 compactness and dry weight, and thus increases the soil water conductivity (Fouli et al., 2013). On this basis,
395 we also found that the freeze/thaw process significantly altered the size and number of soil pores, especially
396 after freezing, and the number of macropores decreased, while the contribution of macropores to the
397 saturated flow decreased. The proportion of the saturated flow in the mesopores with a pore size of <0.3 mm
398 approached or even exceeded the proportion in the macropores, indicating that the soil water inside relatively
399 large pores is more likely to freeze, which in turn creates a large number of small pores, whereas the water
400 transfer process in unfrozen soils primarily relies on the macropores, with obvious differences (Wilson and
401 Luxmoore, 1988;Watson and Luxmoore, 1986). The unsaturated water conductivity of the frozen soils
402 measured in this study was quite low, but under human control (Watanabe and Kugisaki, 2017) or natural
403 conditions in the field (Espeby, 1990), water has been shown to infiltrate frozen soils through macropores as
404 long as the pore size is large enough. Considering that the soil in this experiment was disturbed soil that had
405 been air dried and sieved, although the macropores created by tillage practices (Lipiec et al., 2006) and
406 invertebrate activities (Lavelle et al., 2006) were excluded, due to the inherent heterogeneity of the soil
407 particles, macropores remain in the uniformly filled soil column (Cortis and Berkowitz, 2004;Oswald et al.,
408 1997), and these macropores still played a role in determining the infiltration water flow.
409 There are still only a few studies related to frozen soil macropore flow and pore distribution; consequently,
410 more data should be acquired and more models should be developed to better understand water movement
411 in frozen soil regions. The experiments in this paper are based on repacked soils that were subjected to the
412 first freeze-thaw cycle in the laboratory, and the conclusions may not be comprehensive. In subsequent
413 studies, we will consider applying the methods used in this paper to field experiments to examine the
414 dynamics of the infiltration capacity and pore distribution in nonhomogeneous soils during whole freeze-

thaw periods under real outdoor climatic conditions, such as lower temperatures and more severe freeze-thaw cycles, but the infiltration solution must be carefully selected; as ethylene glycol has low toxicity, to prevent contamination of agricultural soils and crops, a certain concentration of lactose could be considered (Burt and Williams, 1976;Williams and Burt, 1974). At room temperature, an ethylene glycol aqueous solution and water have similar densities and relatively similar viscosities. We have compared these two infiltration solutions in unfrozen soil field experiments, and the infiltration and pore conditions were basically similar, so we still used an aqueous glycol solution in the frozen soil laboratory experiment. Measurements should focus on frozen soil layers at different depths, especially in the vicinity of freezing peaks, and the spatial variability in the distribution of frozen soil pores should be investigated. This work helps to improve the accuracy of simulations such as those of frozen soil water and heat movement or snowmelt water infiltration processes.

5 Conclusions

In this paper, the infiltration capacity of soil columns under four temperature treatments representing various freeze-thaw stages was measured, and the distribution of the pores of various sizes within the soil was calculated based on the measurements by applying an aqueous ethylene glycol solution with a tension infiltrator in the laboratory. The results revealed that for the three types of soils, i.e., black soil, meadow soil and chernozem, the macropores, which accounted for only approximately 0.1% to 0.2% of the soil volume at room temperature, contributed approximately 50% to the saturated flow, and after freezing, the proportion of macropores decreased to 0.05% to 0.1%, while their share of the saturated flow decreased to approximately 30%. Coupled with the even smaller mesopores, the large and medium pores, accounting for approximately 1% to 2% of the soil volume, conducted almost all of the soil moisture under saturated conditions. Freezing decreased the number of macropores and increased the number of smaller-sized

mesopores, thereby significantly increasing their contribution to the frozen soil infiltration capacity so that the latter was no longer solely dependent on the macropores. The infiltration parameters and pore distribution of the black soil were the least affected by the different negative freezing temperatures under the same moisture content and weight capacity conditions, while those of the meadow soil were the most impacted.

Data availability

Data used in this study are available at Figshare (doi: 10.6084/m9.figshare.12965123).

Author contributions

Ruiqi Jiang designed the research program. Tianxiao Li and Ruiqi Jiang built and deployed the soil column and instruments with assistance from Qinglin Li and Renjie Hou. Dong Liu and Qiang Fu provided funding for test equipment. Song Cui collected soil samples in the field. Ruiqi Jiang and Tianxiao Li analyzed the laboratory data. Ruiqi Jiang prepared the manuscript with comments from Tianxiao Li and Dong Liu.

Competing interests

The authors declare that they have no conflicts of interest

Acknowledgements

We acknowledge that this research was supported by the National Natural Science Foundation of China (51679039), the National Science Fund for Distinguished Young Scholars (51825901), the Heilongjiang Provincial Science Fund for Distinguished Young Scholars (YQ2020E002),"Young Talents" Project of Northeast Agricultural University(18QC28), and the China Postdoctoral Science Foundation Grant (2019M651247).

References

Andersland, O. B., Wiggert, D. C., and Davies, S. H.: Hydraulic conductivity of frozen granular soils, J Environ Eng, 122, 212-216, 10.1061/(ASCE)0733-9372(1996)122:3(212), 1996.

Angulo-Jaramillo, R., Vandervaere, J.-P., Roulier, S., Thony, J.-L., Gaudet, J.-P., and Vauclin, M.: Field measurement of soil surface hydraulic properties by disc and ring infiltrometers: A review and recent developments, Soil and Tillage Research, 55, 1-29, 10.1016/S0167-1987(00)00098-2, 2000.

Ankeny, M. D., Ahmed, M., Kaspar, T. C., and Horton, R.: Simple field method for determining unsaturated hydraulic conductivity, Soil Sci Soc Am J, 55, 467-470, 10.2136/sssaj1991.03615995005500020028x, 1991.

Azmatch, T. F., Sego, D. C., Arenson, L. U., and Biggar, K. W.: Using soil freezing characteristic curve to estimate the hydraulic conductivity function of partially frozen soils, Cold Reg. Sci. Technol, 83, 103-109, 10.1016/j.coldregions.2012.07.002, 2012.

Beven, K., and Germann, P.: Macropores and water flow in soils revisited, Water Resour Res, 49, 3071-3092, 10.1002/wrcr.20156, 2013.

Bodhinayake, W., Si, B. C., and Xiao, C.: New method for determining water‐conducting macro‐and mesoporosity from tension infiltrometer, Soil Sci Soc Am J, 68, 760-769, 10.2136/sssaj2004.0760, 2004.

Bureau, H. L. A.: Heilongjiang soil, Agriculture Press, Beijing, 1992.

Burt, T., and Williams, P. J.: Hydraulic conductivity in frozen soils, Earth Surface Processes, 1, 349-360, 10.1002/esp.3290010404, 1976.

Campbell, G. S.: Soil physics with BASIC: transport models for soil-plant systems, Elsevier, Amsterdam, 1985.

Cheng, Q., Xu, Q., Cheng, X., Yu, S., Wang, Z., Sun, Y., Yan, X., and Jones, S. B.: In-situ estimation of unsaturated hydraulic conductivity in freezing soil using improved field data and inverse numerical modeling, Agr Forest Meteorol, 279, 107746, 10.1016/j.agrformet.2019.107746, 2019.

Cortis, A., and Berkowitz, B.: Anomalous transport in “classical” soil and sand columns, Soil Sci Soc Am

J, 68, 1539-1548, 10.2136/sssaj2004.1539, 2004.

Daniel, Stadler, and, Hannes, Flühler, and, Per-Erik, and Jansson: Modelling vertical and lateral water flow in frozen and sloped forest soil plots, Cold Regions Science & Technology, 10.1016/S0165-232X(97)00017-7, 1997.

Demand, D., Selker, J. S., and Weiler, M.: Influences of macropores on infiltration into seasonally frozen soil, Vadose Zone J, 18, 1-14, 10.2136/vzj2018.08.0147, 2019.

Espeby, B.: Tracing the origin of natural waters in a glacial till slope during snowmelt, J Hydrol, 118, 107-127, 10.1016/0022-1694(90)90253-T, 1990.

Flerchinger, G. N., and Saxton, K. E.: Simultaneous Heat and Water Model of a Freezing Snow-Residue-Soil System I. Theory and Development, American Society of Agricultural Engineers, 10.13031/2013.31041, 1989.

Fouli, Y., Cade-Menun, B. J., and Cutforth, H. W.: Freeze–thaw cycles and soil water content effects on infiltration rate of three Saskatchewan soils, Can J Soil Sci, 93, 485-496, 10.4141/CJSS2012-060, 2013.

Fu, Q., Zhao, H., Li, T., Hou, R., Liu, D., Ji, Y., Zhou, Z., and Yang, L.: Effects of biochar addition on soil hydraulic properties before and after freezing-thawing, Catena, 176, 112-124, 10.1016/j.catena.2019.01.008, 2019.

Gao, B., Yang, D., Qin, Y., Wang, Y., Li, H., Zhang, Y., and Zhang, T.: Change in frozen soils and its effect on regional hydrology, upper Heihe basin, northeastern Qinghai-Tibetan Plateau, Cryosphere, 12, 657-673, 2018.

Gao, H., and Shao, M.: Effects of temperature changes on soil hydraulic properties, Soil Till Res, 153, 10.1016/j.still.2015.05.003, 2015.

Gardner, W.: Some steady-state solutions of the unsaturated moisture flow equation with application to

503 evaporation from a water table, Soil Sci, 85, 228-232, 10.1097/00010694-195804000-00006, 1958.
504 Granger, R. J., Gray, D. M., and Dyck, G. E.: Snowmelt infiltration to frozen Prairie soils, Can J Earth Sci,
505 21, 669-677, 10.1139/e84-073, 1984.
506 Grevers, M., JONG, E. D., and St. Arnaud, R.: The characterization of soil macroporosity with CT
507 scanning, Can J Soil Sci, 69, 629-637, 10.4141/cjss89-062, 1989.
508 Harlan, R.: Analysis of coupled heat‐fluid transport in partially frozen soil, Water Resour Res, 9, 1314-
509 1323, 10.1029/WR009i005p01314, 1973.
510 Hayashi, M., Kamp, G. V. D., and Schmidt, R.: Focused infiltration of snowmelt water in partially frozen
511 soil under small depressions, J Hydrol, 270, 214-229, 10.1016/S0022-1694(02)00287-1, 2003.
512 Hayashi, M.: The Cold Vadose Zone: Hydrological and Ecological Significance of Frozen-Soil Processes,
513 Vadose Zone J, 12, 10.2136/vzj2013.03.0064, 2013.
514 Hussen, A., and Warrick, A.: Alternative analyses of hydraulic data from disc tension infiltrometers, Water
515 Resour Res, 29, 4103-4108, 10.1029/93WR02404, 1993.
516 Jarvis, N.: A review of non‐equilibrium water flow and solute transport in soil macropores: Principles,
517 controlling factors and consequences for water quality, Eur J Soil Sci, 58, 523-546, 10.1111/j.1365-
518 2389.2007.00915.x, 2007.
519 Kamp, G. v. d., Hayashi, M., and Gallén, D.: Comparing the hydrology of grassed and cultivated
520 catchments in the semi-arid Canadian prairies, Hydrol Process, 10.1002/hyp.1157, 2003.
521 Konrad, J.-M., and Morgenstern, N. R.: A mechanistic theory of ice lens formation in fine-grained soils,
522 Can Geotech J, 17, 473-486, 10.1139/t80-056, 1980.
523 Lavelle, P., Decaëns, T., Aubert, M., Barot, S. b., Blouin, M., Bureau, F., Margerie, P., Mora, P., and Rossi,
524 J.-P.: Soil invertebrates and ecosystem services, Eur J Soil Biol, 42, S3-S15, 10.1016/j.ejsobi.2006.10.002, 2006.

Lewis, J., and Sjöstrom, J.: Optimizing the experimental design of soil columns in saturated and unsaturated transport experiments, J Contam Hydrol, 115, 1-13, 2010.

Lipiec, J., Kuś, J., Słowińska-Jurkiewicz, A., and Nosalewicz, A.: Soil porosity and water infiltration as influenced by tillage methods, Soil and Tillage research, 89, 210-220, 10.1016/j.still.2005.07.012, 2006.

Lu, N., and Likos, W. J.: Unsaturated soil mechanics, Wiley, Hoboken, 2004.

Lundin, L.-C.: Hydraulic properties in an operational model of frozen soil, J Hydrol, 118, 289-310, 10.1016/0022-1694(90)90264-X, 1990.

Luxmoore, R.: Micro-, meso-, and macroporosity of soil, Soil Sci Soc Am J, 45, 671-672, 10.2136/sssaj1981.03615995004500030051x, 1981.

McCauley, C. A., White, D. M., Lilly, M. R., and Nyman, D. M.: A comparison of hydraulic conductivities, permeabilities and infiltration rates in frozen and unfrozen soils, Cold Reg. Sci. Technol, 34, 117-125, 10.1016/S0165-232X(01)00064-7, 2002.

Mohammed, A. A., Kurylyk, B. L., Cey, E. E., and Hayashi, M.: Snowmelt infiltration and macropore flow in frozen soils: Overview, knowledge gaps, and a conceptual framework, Vadose Zone J, 17, 1-15, 10.2136/vzj2018.04.0084, 2018.

Mohammed, A. A., Pavlovskii, I., Cey, E. E., and Hayashi, M.: Effects of preferential flow on snowmelt partitioning and groundwater recharge in frozen soils, Hydrol Earth Syst Sc, 23, 5017-5031, 10.5194/hess-23-5017-2019, 2019.

Nimmo, J. R.: Theory for Source-Responsive and Free-Surface Film Modeling of Unsaturated Flow, Vadose Zone J, 9, 295-306, 10.2136/vzj2009.0085, 2010.

Nimmo, J. R.: Preferential flow occurs in unsaturated conditions, Hydrol Process, 26, 786-789, 10.1002/hyp.8380, 2012.

547 Nixon, J.: Discrete ice lens theory for frost heave in soils, Can Geotech J, 28, 843-859, 10.1139/t91-102,
548 1991.
549 Oswald, S., Kinzelbach, W., Greiner, A., and Brix, G.: Observation of flow and transport processes in
550 artificial porous media via magnetic resonance imaging in three dimensions, Geoderma, 80, 417-429,
551 10.1016/S0016-7061(97)00064-5, 1997.
552 Oztas, T., and Fayetorbay, F.: Effect of freezing and thawing processes on soil aggregate stability, Catena,
553 52, 1-8, 10.1016/S0341-8162(02)00177-7, 2003.
554 Peng, X., Frauenfeld, O. W., Cao, B., Wang, K., Wang, H., Su, H., Huang, Z., Yue, D., and Zhang, T.:
555 Response of changes in seasonal soil freeze/thaw state to climate change from 1950 to 2010 across china,
556 Journal of Geophysical Research Earth Surface, 10.1002/2016JF003876, 2016.
557 Perroux, K. M., and White, I.: Designs for Disc Permeameters, Soil Sci Soc Am J, 52, 1205-1215,
558 10.2136/sssaj1988.03615995005200050001x, 1988.
559 Pittman, F., Mohammed, A., and Cey, E.: Effects of antecedent moisture and macroporosity on infiltration
560 and water flow in frozen soil, Hydrol Process, 34, 795-809, 10.1002/hyp.13629, 2020.
561 Smith, M.: Observations of soil freezing and frost heave at Inuvik, Northwest Territories, Canada, Can J
562 Earth Sci, 22, 283-290, 10.1016/0148-9062(85)90073-7, 1985.
563 Spaans, E. J.: The soil freezing characteristic: Its measurement and similarity to the soil moisture
564 characteristic, 1994.
565 Spaans, E. J., and Baker, J. M.: The soil freezing characteristic: Its measurement and similarity to the soil
566 moisture characteristic, Soil Sci Soc Am J, 60, 13-19, 10.2136/sssaj1996.03615995006000010005x, 1996.
567 Stadler, D., Sta¨ hli, M., Aeby, P., and Flu¨ hler, H.: Dye tracing and image analysis for quantifying water
568 infiltration into frozen soils, Soil Sci Soc Am J, 64, 505-516, 10.2136/sssaj2000.642505x, 2000.

569 Stähli, M., Bayard, D., Wydler, H., and Flühler, H.: Snowmelt Infiltration into Alpine Soils Visualized by
570 Dye Tracer Technique, Arctic Antarctic & Alpine Research, 36, 128-135, 10.1657/1523-
571 0430(2004)036[0128:SIIASV]2.0.CO;2, 2004.
572 Taina, I. A., Heck, R. J., Deen, W., and Ma, E. Y.: Quantification of freeze–thaw related structure in
573 cultivated topsoils using X-ray computer tomography, Can J Soil Sci, 93, 533-553, 10.4141/CJSS2012-044,
574 2013.
575 Tarnawski, V. R., and Wagner, B.: On the prediction of hydraulic conductivity of frozen soils, Can Geotech
576 J, 33, 176-180, 10.1139/t96-033, 1996.
577 Wang, D., Yates, S., and Ernst, F.: Determining soil hydraulic properties using tension infiltrometers, time
578 domain reflectometry, and tensiometers, Soil Sci Soc Am J, 62, 318-325,
579 10.2136/sssaj1998.03615995006200020004x 1998.
580 Wang, X., Chen, R., Liu, G., Yang, Y., Song, Y., Liu, J., Liu, Z., Han, C., Liu, X., Guo, S., Wang, L., and
581 Zheng, Q.: Spatial distributions and temporal variations of the near-surface soil freeze state across China under
582 climate change, Global Planet Change, 172, 150-158, 10.1016/j.gloplacha.2018.09.016, 2019.
583 Watanabe, K., and Flury, M.: Capillary bundle model of hydraulic conductivity for frozen soil, Water
584 Resour Res, 44, 10.1029/2008WR007012, 2008.
585 Watanabe, K., and Wake, T.: Hydraulic conductivity in frozen unsaturated soil, Proceedings of the 9th
586 International Conference on Permafrost, 2008, 1927-1932,
587 Watanabe, K., Kito, T., Dun, S., Wu, J. Q., Greer, R. C., and Flury, M.: Water infiltration into a frozen soil
588 with simultaneous melting of the frozen layer, Vadose Zone J, 12, vzj2011.0188, 10.2136/vzj2011.0188, 2013.
589 Watanabe, K., and Kugisaki, Y.: Effect of macropores on soil freezing and thawing with infiltration, Hydrol
590 Process, 31, 270-278, 10.1002/hyp.10939, 2017.

Watanabe, K., and Osada, Y.: Simultaneous measurement of unfrozen water content and hydraulic conductivity of partially frozen soil near 0 C, Cold Reg. Sci. Technol, 142, 79-84, 10.1016/j.coldregions.2017.08.002, 2017.

Watson, K., and Luxmoore, R.: Estimating macroporosity in a forest watershed by use of a tension infiltrometer, Soil Sci Soc Am J, 50, 578-582, 10.2136/sssaj1986.03615995005000030007x, 1986.

Williams, P., and Burt, T.: Measurement of hydraulic conductivity of frozen soils, Can Geotech J, 11, 647-650, 10.1139/t74-066, 1974.

Williams, P. J., and Smith, M. W.: The frozen earth: fundamentals of geocryology, Cambridge University Press, 1989.

Wilson, G., and Luxmoore, R.: Infiltration, macroporosity, and mesoporosity distributions on two forested watersheds, Soil Sci Soc Am J, 52, 329-335, 10.2136/sssaj1988.03615995005200020005x, 1988.

Wooding, R.: Steady infiltration from a shallow circular pond, Water Resour Res, 4, 1259-1273, 10.1029/WR004i006p01259, 1968.

Zhao, Y., Nishimura, T., Hill, R., and Miyazaki, T.: Determining hydraulic conductivity for air‐filled porosity in an unsaturated frozen soil by the multistep outflow method, Vadose Zone J, 12, 1-10, 10.2136/vzj2012.0061, 2013.